Representing sub-grid scale variations in nitrogen deposition associated with land use in a global Earth System Model: implications for present and future nitrogen deposition fluxes over North America

Fabien Paulot[1,2], Sergey Malyshev[1], Tran Nguyen[3], John D. Crounse[4],
Elena Shevliakova[1], and Larry W. Horowitz[1]

[1]Geophysical Fluid Dynamics Laboratory, National Oceanic and Atmospheric Administration,
Princeton, New Jersey, USA
[2]Program in Atmospheric and Oceanic Sciences, Princeton University, New Jersey, USA
[3]Department of Environmental Toxicology, UC Davis, Davis, California, USA
[4]Division of Geological and Planetary Sciences, Caltech, Pasadena, California, USA

Correspondence to: Fabien.Paulot@noaa.gov

Abstract. Reactive nitrogen (N) emissions have increased over the last 150 years as a result of greater fossil fuel combustion and food production. The resulting increase in N deposition can alter the function of ecosystems, but characterizing its ecological impacts remains challenging, in part because of uncertainties in model-based estimates of N dry deposition. Here, we leverage the

5   tiled structure of the land component (LM3) of the Geophysical Fluid Dynamics Laboratory (GFDL) Earth System Model to represent the impact of physical, hydrological, and ecological heterogeneities on the surface removal of chemical tracers. We show that this framework can be used to estimate N deposition at more ecologically-relevant scales (e.g., natural vegetation, water bodies) than from the coarse-resolution global chemistry–climate model (GFDL-AM3). Focusing on North America, we

10   show that the faster removal of N over forested ecosystems relative to cropland and pasture implies that coarse resolution estimates of N deposition from global models systematically underestimate N deposition to natural vegetation by 10 to 30% in the Central and Eastern US. Neglecting the subgrid scale heterogeneity of dry deposition velocities also results in an underestimate (overestimate) of the amount of reduced (oxidized) nitrogen deposited to water bodies. Overall, changes in land cover

15   associated with human activities are found to slow down the removal of N from the atmosphere, causing a reduction in the dry oxidized, dry reduced, and total N deposition over the contiguous US of 8%, 26%, and 6%, respectively. We also find that the reduction in the overall rate of removal of N associated with land-use change tends to increase N deposition on the remaining natural vegetation and facilitate N export to Canada. We show that subgrid scale differences in the surface removal

20   of oxidized and reduced nitrogen imply that near-term (2010–2050) changes in oxidized (-47%)

and reduced (+40%) US N emissions will cause opposite changes in N deposition to water bodies (increase) and natural vegetation (decrease) in the Eastern US, with potential implications for acidification and ecosystems.

1 Introduction

Fossil fuel combustion and food production release reactive nitrogen (N) to the atmosphere (Fowler et al., 2013). Once in the atmosphere, N can be transported over long distances before it is removed by dry and wet deposition, providing greater N inputs to otherwise pristine regions (e.g., national parks, boreal forests) (Paulot et al., 2014; Malm et al., 2016). Since N can be a limiting nutrient, the increase in N deposition may promote ecosystem productivity, (Townsend et al., 1996; Magnani et al., 2007; Pregitzer et al., 2008; Reay et al., 2008; Dezi et al., 2010; Wårlind et al., 2014; Devaraju et al., 2015) especially in boreal regions (Högberg, 2012; Gundale et al., 2014; Fleischer et al., 2015). Increasing N deposition can also cause adverse environmental impacts for terrestrial ecosystems including soil acidification, loss of biodiversity, and eutrophication (Stevens et al., 2004; Bobbink et al., 2010; Sutton et al., 2011; Pardo et al., 2011; Sheppard et al., 2011; Phoenix et al., 2012; Erisman et al., 2013; de Vries et al., 2015; Simkin et al., 2016). In the US, oxidized N deposition is projected to decrease as a result of effective controls on NO emissions, but deposition of reduced N ($NH_x \equiv NH_3 + NH_4^+$), primarily from agricultural emissions of NH_3, is projected to remain elevated or even increase (Dentener et al., 2006; Ellis et al., 2013; Paulot et al., 2013; Lamarque et al., 2013; Li et al., 2016). This raises concerns of irreversible damages to sensitive biomes (Pardo et al., 2011; Meunier et al., 2016; Grizzetti, 2011; Dise, 2011), such as high-elevation lakes (Wolfe et al., 2003; Baron et al., 2012; Lepori and Keck, 2012), and organisms (e.g., lichen (Johansson et al., 2012)).

Significant challenges remain in quantifying the long-term impacts of N deposition on ecosystems in a changing climate (Sutton et al., 2008; Wu and Driscoll, 2010; Phoenix et al., 2012; Högberg, 2012; de Vries et al., 2015; Storkey et al., 2015), including uncertainties in the magnitude and spatial distribution of the N deposition flux itself (Sutton et al., 2008; Ochoa-Hueso et al., 2011; Fleischer et al., 2013). N is removed from the atmosphere by wet (i.e., precipitation) and dry (i.e., surface) deposition (Dentener et al., 2006). Much progress has been achieved in characterizing present-day N deposition by using high-resolution chemical transport model combined with observed N fluxes and atmospheric concentrations (e.g. using the Community Multiscale Air Quality Modeling System (Schwede and Lear, 2014; Bytnerowicz et al., 2015; Williams et al., 2017)). However, the requirement for observations and the elevated computational requirement associated with high-resolution atmospheric models limit the applicability of such approach to a few regions (Western Europe and the North America) over limited time periods (mostly post 2000). In particular, assessments of the long-term impact of N deposition on ecosystems, its sensitivity to climate change, and ultimately its coupling with the carbon cycle (Smith et al., 2014; Zaehle et al., 2010; Fleischer et al., 2013;

Dirnböck et al., 2017; Fleischer et al., 2015) require estimates of historical and future N deposition derived from global chemistry-climate models (e,g, Dentener et al. (2006); Lamarque et al. (2013)). However, the coarse resolution ($\simeq$ 100km) of such models may introduce significant biases in N dry deposition fluxes.

60   The goal of this study is to develop a framework to diagnose ecosystem-specific N dry deposition fluxes within a global chemistry climate model on decadal to centenial time scales. First we describe the coupling of the Geophysical Fluid Dynamics Laboratory (GFDL) land-model (LM3) to the GFDL atmospheric chemistry–climate model (AM3) to represent the impact of natural (e.g., vegetation type, soil and canopy wetness) and man-made (e.g., deforestation, cropping) heterogeneities

65   on dry deposition. We then show that the tiled structure of LM3 can be leveraged to derive N deposition on a more ecologically-relevant scale (e.g., deposition on water bodies or natural vegetation). Finally, we discuss how this framework can be used to better represent the impact of land-use change and future trends in N emissions on N deposition.

2   Methods

2.1   Model description

70

We use the GFDL AM3 atmospheric chemistry–climate model (Donner et al., 2011; Naik et al., 2013; Paulot et al., 2016) to simulate atmospheric dynamics and chemistry. Except for the treatment of dry deposition, the model configuration is identical to the one recently described by Paulot et al. (2016) and Paulot et al. (2017), including updates to wet deposition and the chemistry of sulfate and

75   nitrate. The horizontal resolution of the model is 200km with 48 vertical levels.

In previous versions of AM3, the surface removal of chemical tracers was calculated using a prescribed monthly climatology of dry deposition velocities (Naik et al., 2013; Paulot et al., 2016). The lack of a dynamic representation of dry deposition reduces the ability of the model to capture the impact of past and future variability in environmental conditions (e.g., drought (Wu et al., 2016),

80   climate change) and land-use change on atmospheric chemistry. We note that these limitations are not specific to AM3 but affect all chemical transport models that do not include a comprehensive land model (Ellis et al., 2013; Ran et al., 2017).

Here, we use the GFDL land model (LM3) (Shevliakova et al., 2009; Milly et al., 2014) to represent the impact of surface properties on dry deposition. LM3 is a comprehensive climate land-model

85   that includes detailed representations of vegetation dynamics and hydrology and is designed to be run over decadal to century time scales under both historical and future conditions. The combined model will be referred to as AM3-LM3-DD hereafter.

LM3 can be run both coupled with AM3 and in standalone mode with prescribed meteorological fields (Milly et al., 2014). In LM3, land use is represented using a sub-grid mosaic of tiles.

90   Each tile represents a different land type including water bodies, glacier, and four kinds of land-use

types: cropland, pasture, secondary vegetation, i.e. vegetation in a state of recovery after logging or abandonment of pasture and cropland, and undisturbed vegetation, hereafter referred to as natural vegetation (Shevliakova et al., 2009; Malyshev et al., 2015). The spatial distribution and spatial extent of water bodies and glaciers are time–invariant. The transition rates among vegetated tiles are

95 based on the Coupled Model Intercomparison Project, phase 5 (CMIP5) historical reconstructions of land-use up to 2005 and projections from integrated assessment models for 2005 to 2100 (Hurtt et al., 2011). The history of land disturbances is represented by up to 10 secondary tiles per grid cell. Each land tile has distinct physical, hydrological, and ecological properties (Milly et al., 2014). Land properties that affect the surface removal of chemical tracers, such as snow cover, canopy wetness,

100 surface and canopy temperature, leaf area index (LAI), stomatal conductance, and vegetation height are all prognostic (Malyshev et al., 2015). Each vegetated tile has a unique vegetation type (C3 grass, C4 grass, temperate deciduous, coniferous, or tropical vegetation), which is determined based on environmental conditions as well as management for pasture (grazing) and cropland (planting and harvesting). The representation of management practices is important in determining the impact

105 of land-use change on dry deposition, as it affects the vegetation type, and the seasonality of the vegetation cover. In LM3, crop harvesting and pasture grazing are performed annually at the end of the calendar year (Malyshev et al., 2015). Previous work has shown that this treatment contributes to an underestimate of the impact of management on land cover (Malyshev et al., 2015) and we make the following revisions. For pasture, we assume that 25% of leaf biomass is removed daily by grazing,

110 provided LAI exceeds 2 to avoid overgrazing. This higher grazing frequency prevents the growth of trees in the tropics and mid latitudes on pasture, a problem which was noted in previous versions of LM3 (Malyshev et al., 2015). For crops, we specify planting and harvesting dates from the global monthly irrigated and rainfed crop areas climatology (Portmann et al., 2010).

The tiled structure of LM3 is especially useful to diagnose fluxes to areas, such as natural veg-

115 etations or water bodies, which are generally not well-represented by the average properties of the grid-box, in which they are located, because of their small geographical extent (Fig. S1).

The dry deposition velocity ($v_d(X)$) for a compound X is calculated independently for each tile following the widely used electrical circuit analogy (Fig. 1) (Hicks et al., 1987; Wesely, 1989; Zhang et al., 2001, 2003).

$$v_d(X) = \left[R_a + \cfrac{1}{\cfrac{1}{R_{ac,g} + R_{b,g}(X) + R_{sf,g}(X)} + \cfrac{1}{R_{ac,v} + \cfrac{1}{[R_{b,s} + R_{sf,s}]^{-1} + \cfrac{1}{R_{b,v} + \left[R_{sf,v}^{-1} + (R_m + R_s)^{-1}\right]^{-1}}}}} \right]^{-1}$$

120

$$(1)$$

Briefly, the aerodynamic resistance (R_a) to the exchange of tracers between the canopy and the atmosphere is determined using Monin-Obukhov similarity theory. The aerodynamic conductance to the ground ($R_{ac,g}$) and to the vegetation ($R_{ac,v}$) are independent of the chemical tracer and taken from Erisman (1994) and Bonan (1996), respectively. We focus next on the representation of the dry

125 deposition of gases, which is much faster than that of fine particles (Zhang et al., 2002).

Following Jensen and Hummelshøj (1995) and Jensen and Hummelshøj (1997), the canopy laminar resistance ($R_{b,v}$) is defined as:

$$R_{b,v}(X) = \frac{1}{D_X} \left(\frac{u_\star}{\nu} LAI \right)^{-2/3} (100lw)^{1/3} \tag{2}$$

where $u_\star$ is the friction velocity, lw the leaf width (Table S1), LAI the leaf area index, ν the kine-

130 matic viscosity, and D_X the diffusivity of X. Following Hicks et al. (1987), the stem laminar resistance is:

$$R_{b,s}(X) = \frac{2}{\kappa u_\star} \left(\frac{Sc(X)}{Pr} \right)^{2/3} \tag{3}$$

where Pr is the Prandtl number, $Sc(X)$ is the Schmidt number, the ratio of the kinematic to the mass diffusivity ($Sc \propto D_X^{-1}$), κ the von Karman constant ($\kappa = 0.4$). Similarly, the ground surface

135 laminar resistance is:

$$R_{b,g}(X) = \frac{2}{\kappa u_{g\star}} \left(\frac{Sc(X)}{Pr} \right)^{2/3} \tag{4}$$

where $u_{g\star}$ is the friction velocity near the ground (Loubet et al., 2006). The stomatal resistance ($R_s X$) is calculated as

$$R_s(X) = \sqrt{\frac{M(X)}{M(\text{H}_2\text{O})}} R_s(\text{H}_2\text{O}) \tag{5}$$

140 where $M(X)$ is the molecular weight of X and $R_s(\text{H}_2\text{O})$ is calculated according to the Ball-Berry-Leuning model (Leuning, 1995; Milly et al., 2014). This model accounts for the impact of water stress and CO_2 concentration, two factors that are not included in many atmospheric chemistry models (Wesely, 1989; Wang et al., 1998; Emmons et al., 2010) but have been shown to modulate the response of surface ozone to drought (Huang et al., 2016) and CO_2 increase (Sanderson et al.,

145 2007). Cuticle (v), stem (s), and ground (g) resistances for species X are parameterized based on SO_2 and O_3:

$$R_{sf,i}(X) = \frac{s(T)}{\gamma(X)} \left(\frac{\alpha(X)}{R_{sf,i}(\text{SO}_2)} + \frac{\beta(X)}{R_{sf,i}(\text{O}_3)} \right)^{-1} \qquad i \in \{\text{v, s, g}\} \tag{6}$$

where $R_{sf,i}(SO_2)$ and $R_{sf,i}(O3)$ are tabulated resistances (Table S1) for each surface type, and $\alpha(X)$ and $\beta(X)$ are weighting factors (Table S2) estimated using the solubility (for α) and reactivity (for β) of X (Wesely, 1989; Zhang et al., 2002), $s(T)$ is a temperature adjustment factor (Zhang et al., 2003), and $\gamma(X)$ is a codeposition adjustment, which reflects changes in $R_{sf,i}(X)$ associated with surface acidity (Erisman et al., 1994; Massad et al., 2010; Neirynck et al., 2011; Wu et al., 2016). Here, we use a modified version of the parameterizations of Massad et al. (2010) for NH_3 and Simpson et al. (2003) for SO_2:

$$\gamma(X) = \begin{cases} \exp(2 - r_{SN}) & X = SO_2 \text{ and } \alpha_{SN} \leq 2 \\ 6.35 r_{SN} & X = NH3 \\ 1 & \text{otherwise} \end{cases} \tag{7}$$

where $r_{SN} = 0.5 \frac{2DEP(SO_2) + 2DEP(SO4) + DEP(HNO3) + DEP(NO3)}{DEP(NH3) + DEP(NH4)}$ and $DEP(X)$ denotes the dry deposition of X integrated over the previous 24h.

Fig. 2 shows the sensitivity of $v_d(SO_2)$ and $v_d(NH_3)$ to temperature, wetness, and surface acidity in three global models: MOZART (Emmons et al., 2010), GEOS-Chem (Wang et al., 1998), and AM3-LM3–DD. Under dry conditions, GEOS-Chem and AM3-LM3–DD produce identical results for $v_d(SO_2)$, with the temperature dependence driven by that of the stomatal conductance. At low and high temperatures, $v_d(NH_3)$ is faster in AM3-LM3–DD than GEOS-Chem, which reflects small differences in the assumed surface pH (6.35 and 6.6 respectively). In contrast, MOZART assumes a surface pH=5 and accounts for changes in the effective solubility of SO_2 and NH_3 with temperature, similar to Nguyen et al. (2015). The increase in solubility with decreasing temperature results in faster $v_d(X)$ at cold temperature in MOZART, while the lower pH increases $v_d(NH_3)$ and decreases $v_d(SO_2)$. The impact of surface wetness on $v_d(X)$ is only considered in MOZART and AM3-LM3 DD. In MOZART the presence of dew more than doubles $v_d(SO_2)$ but reduces $v_d(NH_3)$ below 25°C. In contrast, both $v_d(NH_3)$ and $v_d(SO_2)$ increase in AM3-LM3–DD when the canopy is wet, which is supported by observations (Erisman et al., 1994, 1999; Massad et al., 2010). AM3-LM3–DD also accounts for the modulation of $R_{sf,v}(SO_2)$ and $R_{sf,v}(NH_3)$ by the acidity of the surface. Our results suggest that when $\alpha_{SN} = 2$, i.e. when the deposition of acids is twice as large as the deposition of bases, the impact of codeposition can be greater than that of canopy wetness. The large differences in the response of $v_d(SO_2)$ and $v_d(NH_3)$ to environmental conditions across three models highlight the need for a more robust understanding of the mechanisms controlling $R_{sf,i}(X)$.

2.2 Experimental design

We perform two sets of global simulations under present-day (2007–2010) and future (2050) conditions. For present-day conditions, AM3-LM3-DD is forced with observed sea surface temperature and sea ice cover. Horizontal winds are nudged to those from the National Centers for Environmental Prediction reanalysis (Kalnay et al., 1996) to minimize meteorological variability across configura-

tions. Anthropogenic emissions are from the Hemispheric Transport of Air Pollution 2 (HTAP 2, Janssens-Maenhout et al. (2015)). For 2050, we use the vegetation, sea surface temperature, and sea ice cover simulated by the GFDL-CM3 model under the Representative Concentration Pathways

185   8.5 scenario (Riahi et al., 2011) in 2050 (Levy et al., 2013). RCP8.5 anthropogenic emissions for 2050 are used (Lamarque et al., 2011) except for NH_3, where we use the spatial distribution and seasonality of HTAPv2 emissions (Janssens-Maenhout et al., 2015) following Paulot et al. (2016). The model is run for 10 years with land-use fixed to year 2050 and we use the average of the last 9 years to minimize the impact of internal variability.

190   ## 3   Results and discussion

3.1   Evaluation

We first evaluate the representation of $v_d(SO_2)$ in AM3-LM3–DD for present-day (2007-2010) using observations collected over a wide range of surfaces. Fig. 3 shows observed and simulated $v_d(SO_2)$ grouped among the four types of vegetation simulated by LM3 (deciduous, coniferous, tropical, and

195   grass). Simulated deposition velocities generally fall within a factor of 2 of the observations, with better agreement during the day than at night, when the model is biased high. The model qualitatively captures the winter to summer increase in $v_d(SO_2)$ over deciduous forests as well as its increase with canopy wetness. However, the model underestimates $v_d(SO_2)$ over grassland. Here, we do not account for the sub-grid heterogeneity of anthropogenic NH_3 emissions, which would likely result in

200   higher NH_3 concentrations and thus faster $v_d(SO_2)$ (Neirynck et al., 2011) over fertilized grasslands (Nemitz et al., 2001; Flechard et al., 2013).

There are fewer observations of the deposition velocity of individual N carriers in part because of measurement challenges (Nguyen et al., 2015). Fig. 4 shows the observed and simulated deposition velocities for HNO_3, a range of organic nitrates (ISOPN, MVKN, PROPNN) derived from isoprene

205   photooxidation (Paulot et al., 2009), and HCN in summer over a mixed forest in the Southeast US. The simulated and observed deposition velocities of H_2O_2 are also shown. We refer the reader to Nguyen et al. (2015) for information regarding the site and Caltech observations.

To facilitate the comparison between simulated and observed deposition velocities, we run LM3 in standalone model using meteorological fields (wind speed, temperature, precipitation, and downward

210   radiation) from the Modern-Era Retrospective Analysis for Research and Applications (MERRA) (Rienecker et al., 2011). The measured compounds have different chemical properties, allowing us to evaluate the representation of different deposition pathways in AM3-LM3–DD. In particular, HNO_3 and H_2O_2 have negligible cuticular resistance ($R_{surf,v} \simeq 0$) (Nguyen et al., 2015), such that $v_d(X) \simeq [R_a + R_{b,v}(X)]^{-1}$ (ground deposition is negligible). The model captures both

215   $v_d(H_2O_2)$ and $v_d(HNO_3)$ well, including the faster deposition of H_2O_2 relative to HNO_3 consistent with the dependence of R_b on $1/D_X \propto \sqrt{MW(X)}$ (equation 2). $v_d(H_2O_2)$ and $v_d(HNO_3)$

are overestimated in the late afternoon and at night. This may reflect excessive mixing in the model during these time periods (i.e., R_a too low). In contrast, the deposition of HCN on cuticles is negligible ($R_{sf,v} \gg 1$ s/m), so that $v_d(\text{HCN}) \simeq R_s(\text{HCN})^{-1}$. Comparison of observed and modeled

220 $v_d(\text{HCN})$ suggests that the Ball-Berry-Leuning model captures the stomatal conductance well at this site. Since R_a, $R_{b,v}$, and R_s are well represented over the measurement period, we use observations of $v_d(\text{ISOPN})$, $v_d(\text{MVKN})$, and $v_d(\text{PROPNN})$ at this site to estimate α and β for these organic nitrates. We find that ($\alpha = 7$, $\beta = 1$) provide a reasonable fit for all organic nitrates and we use these values globally.

225 ## 3.2 Impact of land heterogeneities on present-day N deposition

Fig. 5 shows the simulated dry deposition of oxidized N (dominated by HNO_3) and reduced N (dominated by NH_3) as well as the total N deposition (wet+dry) in North America. As noted in previous studies (Zhang et al., 2012; Lamarque et al., 2013), the overall pattern of N deposition mirrors the underlying distribution of NH_3 and NO emissions, with high deposition in the Northeast

230 and greater contribution of reduced nitrogen to N deposition in the US Midwest than in the Eastern US.

The simulated dry deposition represents the sum of the deposition fluxes to the tiles that comprise each grid cell. Fig. 5 (middle column) shows that N deposition over natural vegetation is generally greater than the grid-cell average, which is consistent with faster deposition velocities over forests

235 relative to grasslands (Finkelstein, 2001; Hicks, 2006) (see supplementary materials). This enhancement is largest in regions that have experienced extensive deforestation (e.g., in the US Northeast) and smallest in regions with little agricultural activity (e.g., most of Canada) or where managed vegetation differs little in height and LAI from natural vegetation (e.g., in the Western US). Fig. 5 (middle column) also shows that the dry deposition of NH_x is more sensitive to land-use change

240 than that of NO_y, which reflects the much faster deposition velocity of HNO_3 relative to NH_3 (Fig. S2). Overall, the simulated total N deposition to natural ecosystems exceeds the grid-box average deposition by 10 to 30% over most of the Eastern and Central US.

Fig. 5 (right column) also shows that water bodies receive more reduced N but less oxidized N through dry deposition than the grid-box average. These differences can be attributed to the large

245 effective solubility of NH_3 in freshwater, which results in lower $R_{sf,g}(\text{NH}_3)$ than over vegetated surfaces ($R_{sf,g}(\text{HNO}_3)$ is low over all surfaces). In contrast, our model suggests that $v_d(\text{HNO}_3)$ is generally slower over water bodies than over vegetated surfaces because of the lower roughness height of water bodies (see Fig. S2). The westward increase in the ratio of NH_3 to NO emissions thus results in water bodies receiving less N than the average grid cell in the Eastern US and Canada

250 but more in the Central and Western US. .

In order to quantify the impact of land-use change on nitrogen deposition, we perform an additional simulation in which only natural vegetation is considered. Fig. 6 shows that anthropogenic

land-use change has decreased dry NO_y, dry NH_x, and total N deposition over the contiguous US
by 8%, 26%, and 6%, respectively. This reflects the reduction in deposition velocity associated with
255 lower LAI and height for crop and pasture relative to natural vegetation. This reduction of the over-
all deposition velocity near source regions tends to increase the surface concentration of N car-
rier, which leads to greater N deposition on the remaining natural vegetation. For instance, Fig. 6
shows that land-use change has induced a 14% decrease of the overall N deposition in the region
of Shenandoah National Park, but an increase of 9% on natural vegetation. The slower removal of
260 N near source regions also facilitates N export to remote regions, such as Eastern Canada, where
N deposition (primarily through wet deposition) increases by more than 10%. This suggests that
anthropogenic land-use change in North America has contributed to the increase of N deposition to
natural ecosystems both near source regions and in remote receptor regions.

3.3   Implications for future N deposition

265 Fig. 7 shows the simulated change in N deposition from 2010 to 2050 in response to changes in
climate, anthropogenic emissions, and land properties induced by climate and land-use change in
the RCP8.5 scenario (van Vuuren et al., 2011; Riahi et al., 2011). In this scenario, the fraction of
land devoted to agriculture decreases in North America (Davies-Barnard et al., 2014), which results
in a small increase of $v_d(HNO_3)$ and a larger increase of $v_d(NH_3)$ (Fig. S3). However, in our model
270 the increase of $v_d(NH_3)$ is compensated by the decrease in acid deposition, which reduces $v_d(NH_3)$
especially in the Eastern US (see equation 7).

Total N deposition is projected to increase by 9% over the contiguous US. Most of the increase is
driven by greater deposition in the Midwest and Western US associated with higher NH_3 emissions
(+40%). In contrast, N deposition is projected to decrease in the Eastern US following the decrease
275 of NO emissions (-47%, mostly in the Eastern US). These trends are amplified over natural vegeta-
tion consistent with faster deposition velocities. Water bodies are projected to experience an increase
in N deposition over most of the US, including in regions which experience an overall decrease in N
deposition. This contrast is driven by the faster removal of NH_3 over water relative to managed veg-
etation, which result in greater sensitivity to changes in the emissions of reduced N. These opposite
280 responses are important for projections of N deposition in national parks, where N deposition to both
vegetation and water bodies is of concern. For instance, the changes in N deposition at Voyageurs
and Shenandoah national parks are 30% greater than simulated in the grid box where they are lo-
cated, while N deposition to water bodies in the Shenandoah region is projected to increase by 16%,
even though overall N deposition decreases by 18% in this region.

285 4 Conclusions

Our study highlights the importance of accounting for surface heterogeneities and anthropogenic land use in modulating the magnitude and trend of N deposition. Here, we leverage the tiled structure of the GFDL land model to efficiently represent the subgrid scale heterogeneity of surface properties and their evolution in a changing climate. We have shown that the shift of N emissions from oxi-
290 dized to reduced N in North America will exacerbate the sensitivity of N deposition to small-scale heterogeneities, which highlights the need to improve the representation of non-stomatal surface resistances ($R_{sf,v}$, $R_{sf,s}$, and $R_{sf,g}$) (Flechard et al., 2013; Wentworth et al., 2016; Wu et al., 2018).

Our approach is best suited to long time scales (decadal to centennial) and is complementary to ongoing efforts to improve the representation of present-day N deposition using a combination of
295 high-resolution model and observations (Schwede and Lear, 2014). Future work will aim at coupling the representation of dry deposition presented here to the N cycle in the GFDL land model (Gerber et al., 2010), which will enable us to represent the bidirectional exchange of NH_3 (Nemitz et al., 2001; Flechard et al., 2013; Bash et al., 2013) and improve our understanding of the impact of N deposition on ecosystems and carbon cycling (Magnani et al., 2007; Janssens et al., 2010; Fleischer
300 et al., 2013, 2015).

Acknowledgement. This study was supported by NOAA Climate Program Office's Atmospheric Chemistry, Carbon Cycle, and Climate program. Caltech observations and JDC were supported by NSF (Grant #AGS-1240604). We thank V. Naik, A. Fiore, and J. Schnell for helpful comments.
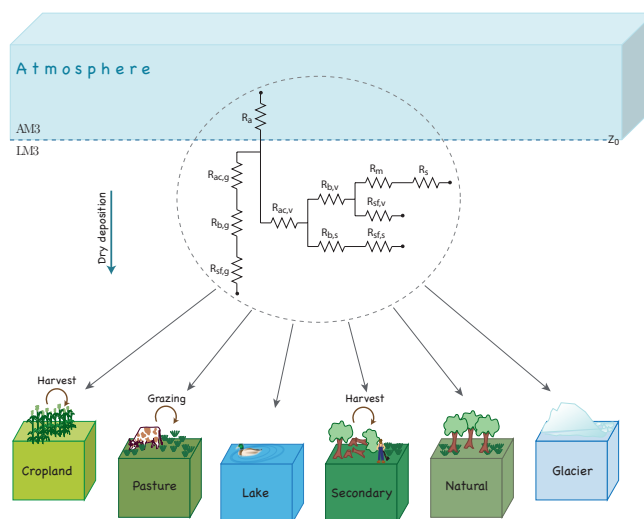
Figure 1. Schematic representation of the resistance scheme used to represent the dry deposition of gaseous tracers for each tile. R_a, $R_{b,i}$, R_{ac}, R_m, R_s, and $R_{sf,i}$ are the aerodynamic resistance, laminar resistance, canopy aerodynamic resistance, mesophyl resistance, stomatal resistance, and surface resistance, respectively. The g, s, and v indexes (i) refer to ground, stem, and vegetation. Note that for clarity deposition on soil and vegetation that are covered by snow or liquid water are not shown.
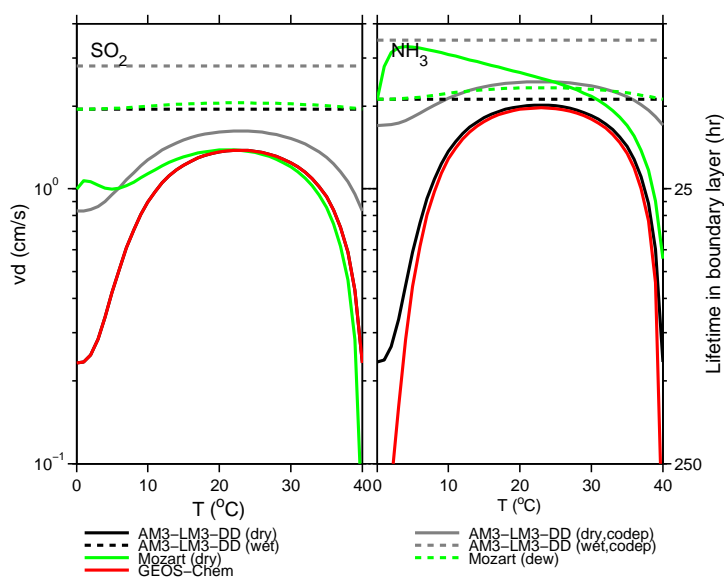
Figure 2. Simulated deposition velocity of NH_3 and SO_2 over a coniferous forest (LAI=5, $u_\star = 0.5$m/s, RH=80%) at different canopy wetness and temperature. To facilitate comparison across models, we use the same $R_a = 20$s/m, R_b (Hicks et al., 1987) and R_s (Wesely, 1989) for all models. Solar irradiation increases linearly from 0 to 800 W/m^2 with temperature. We neglect deposition to the ground and stems. Co-dep refers to the decrease in $R_{sf,v}(SO_2)$ and $R_{sf,v}(NH_3)$ associated with base and acid deposition respectively. For illustrative purposes, the ratio of acid to base deposition is set to 0.5 for SO_2 and 2 for NH_3. The lifetimes of SO_2 and NH_3 are estimated assuming a boundary layer height of 900m. GEOS-Chem and AM3-LM3–DD produce identical results for SO_2 under dry conditions.
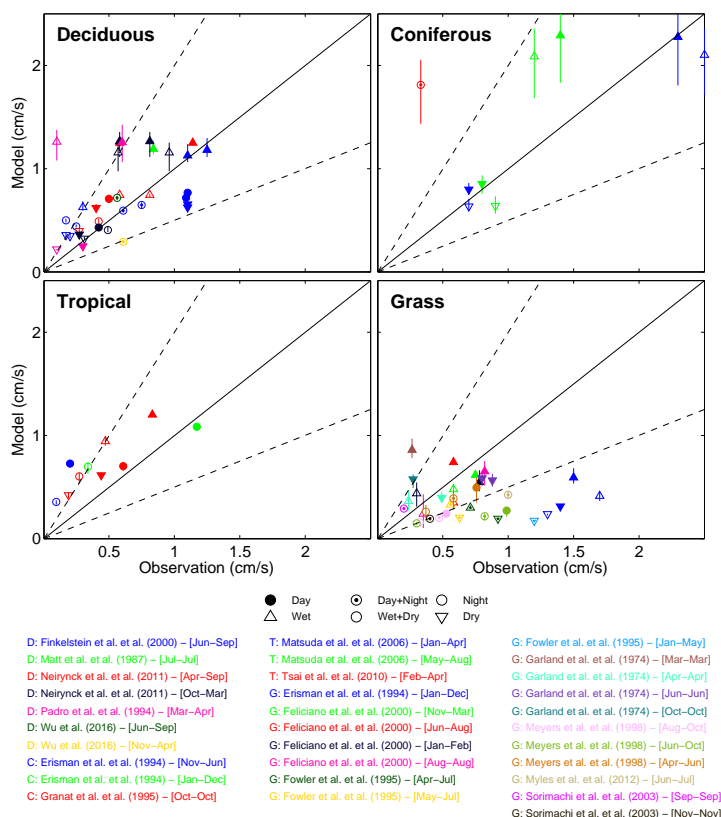
Figure 3. Observed and simulated deposition velocities of SO_2 for different vegetation types. The model is sampled over the same vegetation type and months as the observations. The symbol shape indicates the canopy status: wet (upward pointing triangle), dry (downward point triangle), circle (average). The symbol fill indicates the time period. For comparison with the models, wet conditions are defined as more than 10% of the canopy covered with dew or rain, daytime condition as 10am to 3pm local time, and nightime conditions as 10pm to 5am local time. Reference and time period for each observation are indicated for decidious (D), coniferous (C), tropical (T), and grass (G) (Finkelstein et al., 2000; Matt et al., 1987; Neirynck et al., 2011; Erisman, 1994; Granat and Richter, 1995; Matsuda et al., 2006; Feliciano et al., 2001; Fowler et al., 1995; Garland et al., 1974; Meyers et al., 1998; Myles et al., 2012; Sorimachi et al., 2003; Finkelstein, 2001; Wu et al., 2016).
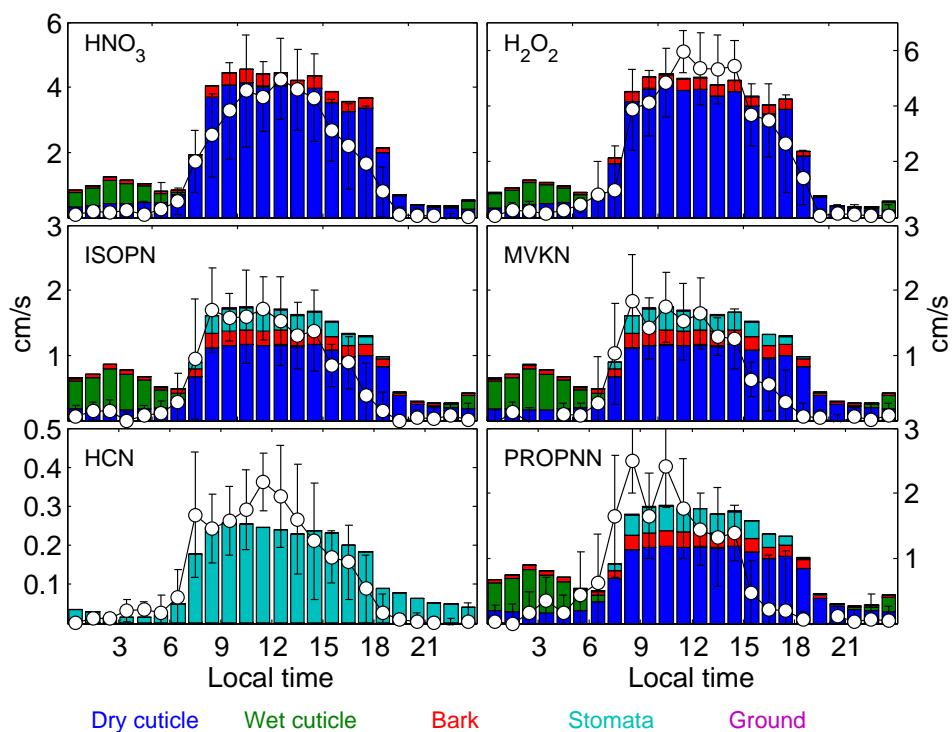
Figure 4. Observed (circles +/- standard deviation) and simulated (bars) dry deposition velocities for several nitrogen–containing species and hydrogen peroxide over the Talladega National Forest (Southeast US) in June 2013 (5 days, Nguyen et al. (2015)). The bar colors indicate the contribution of the different surfaces to the overall surface removal of the chemical tracer.

305
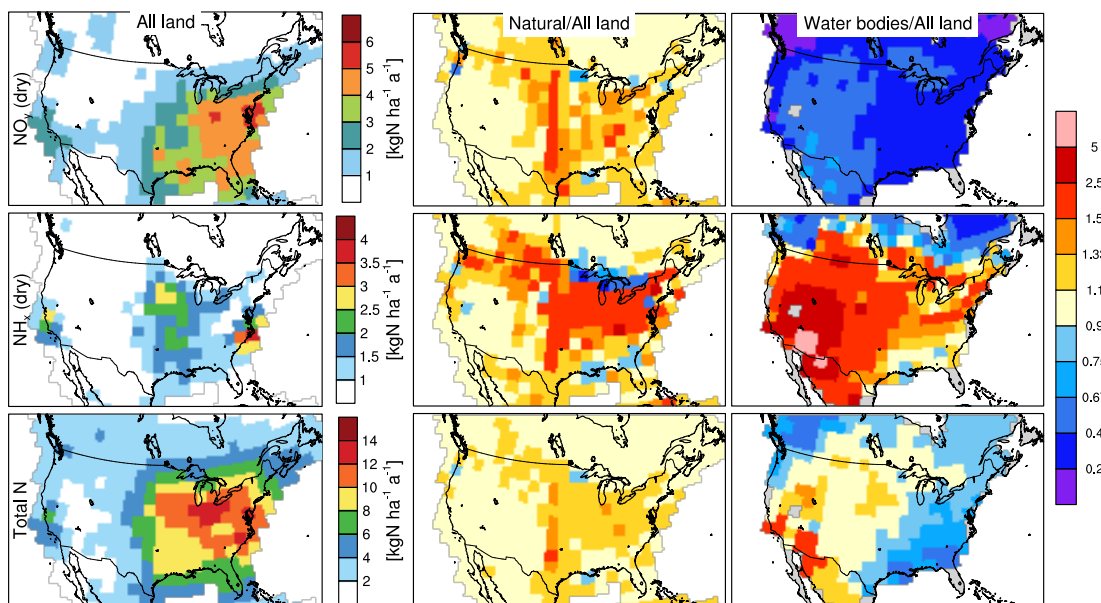
Figure 5. Simulated reactive nitrogen deposition (left column) from dry oxidized nitrogen deposition (first row), dry reduced nitrogen deposition (second row), and total nitrogen deposition (bottom row). The ratio between the deposition on selected land types and the grid cell average deposition is shown in the middle (for natural vegetation) and right columns (water bodies)
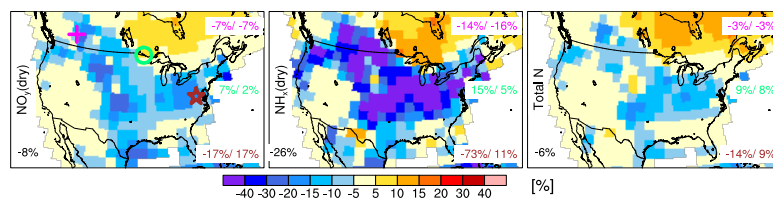
Figure 6. Relative change in the 2008–2010 average land deposition of dry oxidized nitrogen (left), dry reduced nitrogen (center), and total nitrogen (right) associated with anthropogenic land-use change. The relative change is shown as (with land-use - without land land-use)/with land-use. From top right to bottom right, the percentages indicate the change in N deposition at Banff National Park (cross), Voyageurs National Park (circle), and Shenandoah National Park (star) at the grid box level and on natural vegetation, a better proxy for these parks. The fractional change in N deposition over the contiguous US is indicated in inset (bottom left).
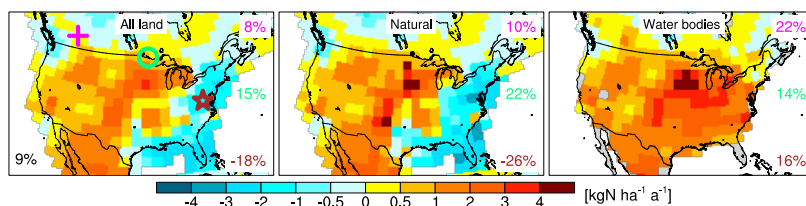
Figure 7. Simulated change in reactive nitrogen deposition from 2010 to 2050 in the RCP8.5 scenario at the grid box level (left), on natural tiles (center) and on water bodies (right). From top right to bottom right, the percentages indicate the change in N deposition at Banff National Park (cross), Voyageurs National Park (circle), and Shenandoah National Park (star) at the grid box level and on natural vegetation tiles respectively. The fractional change in N deposition over the contiguous US is indicated in inset (bottom left).

References

Baron, J. S., Hall, E. K., Nolan, B. T., Finlay, J. C., Bernhardt, E. S., Harrison, J. A., Chan, F., and Boyer, E. W.: The interactive effects of excess reactive nitrogen and climate change on aquatic ecosystems and water resources of the United States, Biogeochemistry, pp. 1–22, 2012.

310 Bash, J. O., Cooter, E. J., Dennis, R. L., Walker, J. T., and Pleim, J. E.: Evaluation of a regional air-quality model with bidirectional NH_3 exchange coupled to an agroecosystem model, Biogeosciences, 10, 1635–1645, 2013.

Bobbink, R., Hicks, K., Galloway, J., Spranger, T., Alkemade, R., Ashmore, M., Bustamante, M., Cinderby, S., Davidson, E., Dentener, F., Emmett, B., Erisman, J.-W., Fenn, M., Gilliam, F., Nordin, A., Pardo, L., and De Vries, W.: Global assessment of nitrogen deposition effects on terrestrial plant diversity: a synthesis,

315 Ecol. Appl., 20, 30–59, 2010.

Bonan, G. B.: Land surface model (LSM version 1.0) for ecological, hydrological, and atmospheric studies: Technical description and users guide. Technical note, Tech. rep., National Center for Atmospheric Research, Boulder, CO (United States). Climate and Global Dynamics Div., 1996.

Bytnerowicz, A., Johnson, R., Zhang, L., Jenerette, G., Fenn, M., Schilling, S., and Gonzalez-Fernandez, I.: An

320 empirical inferential method of estimating nitrogen deposition to Mediterranean-type ecosystems: the San Bernardino Mountains case study, Environmental Pollution, 203, 69–88, doi:10.1016/j.envpol.2015.03.028, https://doi.org/10.1016/j.envpol.2015.03.028, 2015.

Davies-Barnard, T., Valdes, P. J., Singarayer, J. S., Pacifico, F. M., and Jones, C. D.: Full effects of land use change in the representative concentration pathways, Environ. Res. Lett., 9, 114 014, doi:10.1088/1748-

325 9326/9/11/114014, http://stacks.iop.org/1748-9326/9/i=11/a=114014, 2014.

De Schrijver, A., Staelens, J., Wuyts, K., Van Hoydonck, G., Janssen, N., Mertens, J., Gielis, L., Geudens, G., Augusto, L., and Verheyen, K.: Effect of vegetation type on throughfall deposition and seepage flux, Environ. Pollut., 153, 295–303, 2008.

de Vries, W., Hettelingh, J.-P., and Posch, M., eds.: Critical Loads and Dynamic Risk Assessments, vol. 25 of

330 *Environmental Pollution*, Springer Netherlands, Dordrecht, 2015.

Dentener, F., Drevet, J., Lamarque, J. F., Bey, I., Eickhout, B., Fiore, A. M., Hauglustaine, D., Horowitz, L. W., Krol, M., Kulshrestha, U. C., Lawrence, M., Galy-Lacaux, C., Rast, S., Shindell, D., Stevenson, D., Van Noije, T., Atherton, C., Bell, N., Bergman, D., Butler, T., Cofala, J., Collins, B., Doherty, R., Ellingsen, K., Galloway, J., Gauss, M., Montanaro, V., Müller, J. F., Pitari, G., Rodriguez, J., Sanderson, M., Solmon, F.,

335 Strahan, S., Schultz, M., Sudo, K., Szopa, S., and Wild, O.: Nitrogen and sulfur deposition on regional and global scales: A multimodel evaluation, Global Biogeochem. Cycles, 20, B4003, 2006.

Devaraju, N., Bala, G., Caldeira, K., and Nemani, R.: A model based investigation of the relative importance of CO_2-fertilization, climate warming, nitrogen deposition and land use change on the global terrestrial carbon uptake in the historical period, Clim. Dyn., pp. 1–18, 2015.

340 Dezi, S., Medlyn, B. E., Tonon, G., and Magnani, F.: The effect of nitrogen deposition on forest carbon sequestration: a model-based analysis, Glob. Chang. Biol., 16, 1470–1486, 2010.

Dirnböck, T., Foldal, C., Djukic, I., Kobler, J., Haas, E., Kiese, R., and Kitzler, B.: Historic nitrogen deposition determines future climate change effects on nitrogen retention in temperate forests, Climatic Change, 144, 221–235, doi:10.1007/s10584-017-2024-y, https://doi.org/10.1007/s10584-017-2024-y, 2017.

345 Dise, N. B.: The European Nitrogen Assessment: Sources, Effects and Policy Perspectives, chap. 20, Cambridge
     University Press, 2011.

Donner, L. J., Wyman, B. L., Hemler, R. S., Horowitz, L. W., Ming, Y., Zhao, M., Golaz, J.-C., Ginoux, P.,
     Lin, S.-J., Schwarzkopf, M. D., Austin, J., Alaka, G., Cooke, W. F., Delworth, T. L., Freidenreich, S. M.,
     Gordon, C. T., Griffies, S. M., Held, I. M., Hurlin, W. J., Klein, S. A., Knutson, T. R., Langenhorst, A. R.,
350 Lee, H.-C., Lin, Y., Magi, B. I., Malyshev, S. L., Milly, P. C. D., Naik, V., Nath, M. J., Pincus, R., Ploshay,
     J. J., Ramaswamy, V., Seman, C. J., Shevliakova, E., Sirutis, J. J., Stern, W. F., Stouffer, R. J., Wilson, R. J.,
     Winton, M., Wittenberg, A. T., and Zeng, F.: The Dynamical Core, Physical Parameterizations, and Basic
     Simulation Characteristics of the Atmospheric Component AM3 of the GFDL Global Coupled Model CM3,
     J. Clim., 24, 3484–3519, 2011.

355 Ellis, R. A., Jacob, D. J., Sulprizio, M. P., Zhang, L., Holmes, C. D., Schichtel, B. A., Blett, T., Porter, E., Pardo,
     L. H., and Lynch, J. A.: Present and future nitrogen deposition to national parks in the United States: critical
     load exceedances, Atmos. Chem. Phys., 13, 9083–9095, 2013.

Emmons, L. K., Walters, S., Hess, P. G., Lamarque, J.-F., Pfister, G. G., Fillmore, D., Granier, C., Guenther, A.,
     Kinnison, D., Laepple, T., Orlando, J., Tie, X., Tyndall, G., Wiedinmyer, C., Baughcum, S. L., and Kloster,
360 S.: Description and evaluation of the Model for Ozone and Related chemical Tracers, version 4 (MOZART-
     4), Geosci. Model Dev., 3, 43–67, 2010.

Erisman, J. W.: Evaluation of a surface resistance parametrization of sulphur dioxide, Atmos. Environ., 28,
     2583–2594, 1994.

Erisman, J. W., Pul, A. V., and Wyers, P.: Parametrization of surface resistance for the quantifica-
365 tion of atmospheric deposition of acidifying pollutants and ozone, Atmos. Environ., 28, 2595 –
     2607, doi:http://dx.doi.org/10.1016/1352-2310(94)90433-2, http://www.sciencedirect.com/science/article/
     pii/1352231094904332, 1994.

Erisman, J. W., Hogenkamp, J. E. M., Putten, E. M. v., Uiterwijk, J. W., Kemkers, E., Wiese, C. J., and Men-
     nen, M. G.: Long-term Continuous Measurements of SO_2 Dry Deposition over the Speulder Forest, Water.
370 Air. Soil Pollut., 109, 237–262, doi:10.1023/A:1005097722854, http://link.springer.com/article/10.1023/A%
     3A1005097722854, 1999.

Erisman, J. W., Galloway, J. N., Seitzinger, S., Bleeker, A., Dise, N. B., Petrescu, A. M. R., Leach, A. M., and
     Vries, W. d.: Consequences of human modification of the global nitrogen cycle, Phil. Trans. R. Soc. B, 368,
     20130 116, 2013.

375 Fagerli, H. and Aas, W.: Trends of nitrogen in air and precipitation: Model results and observations at EMEP
     sites in Europe, 1980–2003, Environ. Pollut., 154, 448–461, 2008.

Feliciano, M. S., Pio, C. A., and Vermeulen, A. T.: Evaluation of SO_2 dry deposition over short vegetation in
     Portugal, Atmos. Environ., 35, 3633–3643, 2001.

Finkelstein, P. L.: Deposition Velocities of SO_2 and O_3 over Agricultural and Forest Ecosystems, Water, Air
380 and Soil Pollution: Focus, 1, 49–57, 2001.

Finkelstein, P. L., Ellestad, T. G., Clarke, J. F., Meyers, T. P., Schwede, D. B., Hebert, E. O., and Neal, J. A.:
     Ozone and sulfur dioxide dry deposition to forests: Observations and model evaluation, J. Geophys. Res.
     Atmos., 105, 15 365–15 377, 2000.

Flechard, C. R., Massad, R.-S., Loubet, B., Personne, E., Simpson, D., Bash, J. O., Cooter, E. J., Nemitz, E., and
    Sutton, M. A.: Advances in understanding, models and parameterizations of biosphere-atmosphere ammonia
    exchange, Biogeosciences, 10, 5183–5225, 2013.

Fleischer, K., Rebel, K. T., van der Molen, M. K., Erisman, J. W., Wassen, M. J., van Loon, E. E., Montagnani,
    L., Gough, C. M., Herbst, M., Janssens, I. A., Gianelle, D., and Dolman, A. J.: The contribution of nitrogen
    deposition to the photosynthetic capacity of forests, Global Biogeochem. Cycles, 27, 187–199, 2013.

Fleischer, K., Wårlind, D., van der Molen, M. K., Rebel, K. T., Arneth, A., Erisman, J. W., Wassen, M. J.,
    Smith, B., Gough, C. M., Margolis, H. A., Cescatti, A., Montagnani, L., Arain, A., and Dolman, A. J.: Low
    historical nitrogen deposition effect on carbon sequestration in the boreal zone, J. Geophys. Res. Biogeosci.,
    120, 2015JG002 988, 2015.

Fowler, D., Flechard, C., Storeton-West, R. L., Sutton, M. A., Hargreaves, K. J., and Smith, R. I.: Long term
    measurements of SO2 dry deposition over vegetation and soil and comparisons with models, in: Studies in
    Environmental Science, edited by Erisman, G. J. H. a. J. W., vol. 64 of *Acid Rain Research: Do we have
    enough answers?Proceedings of a Specialty Conference*, pp. 9–19, Elsevier, 1995.

Fowler, D., Coyle, M., Skiba, U., Sutton, M. A., Cape, J. N., Reis, S., Sheppard, L. J., Jenkins, A., Grizzetti,
    B., Galloway, J. N., Vitousek, P., Leach, A., Bouwman, A. F., Butterbach-Bahl, K., Dentener, F., Stevenson,
    D., Amann, M., and Voss, M.: The global nitrogen cycle in the twenty-first century, Philos. Trans. R. Soc.
    London, Ser. B, 368, 2013.

Garland, J. A., Atkins, D. H. F., Readings, C. J., and Caughey, S. J.: Deposition of gaseous sulphur dioxide to
    the ground, Atmos. Environ., 8, 75–79, 1974.

Gerber, S., Hedin, L. O., Oppenheimer, M., Pacala, S. W., and Shevliakova, E.: Nitrogen cycling and feedbacks
    in a global dynamic land model, Global Biogeochem. Cycles, 24, GB1001, 2010.

Granat, L. and Richter, A.: Dry deposition to pine of sulphur dioxide and ozone at low concentration, Atmos.
    Environ., 29, 1677–1683, 1995.

Grizzetti, B.: The European Nitrogen Assessment: Sources, Effects and Policy Perspectives, chap. 17, Cam-
    bridge University Press, 2011.

Gundale, M. J., From, F., Bach, L. H., and Nordin, A.: Anthropogenic nitrogen deposition in boreal forests has
    a minor impact on the global carbon cycle, Glob. Chang. Biol., 20, 276–286, 2014.

Hicks, B. B.: Dry deposition to forests—On the use of data from clearings, Agric. For. Meteo-
    rol., 136, 214–221, doi:10.1016/j.agrformet.2004.06.013, http://www.sciencedirect.com/science/article/pii/
    S0168192305002066, 2006.

Hicks, B. B.: On Estimating Dry Deposition Rates in Complex Terrain, Journal of Applied Meteorology and
    Climatology, 47, 1651–1658, 2008.

Hicks, B. B., Baldocchi, D. D., Meyers, T. P., Hosker, R. P., and Matt, D. R.: A preliminary multiple resistance
    routine for deriving dry deposition velocities from measured quantities, Water, Air, & Soil Pollution, 36,
    311–330, 1987.

Högberg, P.: What is the quantitative relation between nitrogen deposition and forest carbon sequestration?,
    Glob. Chang. Biol., 18, 1–2, 2012.

Huang, L., McDonald-Buller, E. C., McGaughey, G., Kimura, Y., and Allen, D. T.: The im-
    pact of drought on ozone dry deposition over eastern Texas, Atmos. Environ., 127, 176–

186,   doi:10.1016/j.atmosenv.2015.12.022,   http://www.sciencedirect.com/science/article/pii/
425   S1352231015305902, 2016.

Hurtt, G. C., Chini, L. P., Frolking, S., Betts, R. A., Feddema, J., Fischer, G., Fisk, J. P., Hibbard, K., Houghton,
R. A., Janetos, A., Jones, C. D., Kindermann, G., Kinoshita, T., Goldewijk, K. K., Riahi, K., Shevliakova,
E., Smith, S., Stehfest, E., Thomson, A., Thornton, P., Vuuren, D. P. v., and Wang, Y. P.: Harmonization of
land-use scenarios for the period 1500–2100: 600 years of global gridded annual land-use transitions, wood
430   harvest, and resulting secondary lands, Clim. Change, 109, 117–161, 2011.

Janssens, I. A., Dieleman, W., Luyssaert, S., Subke, J.-A., Reichstein, M., Ceulemans, R., Ciais, P., Dolman,
A. J., Grace, J., Matteucci, G., Papale, D., Piao, S. L., Schulze, E.-D., Tang, J., and Law, B.: Reduction of
forest soil respiration in response to nitrogen deposition, Nature Geosci, 3, 315–322, 2010.

Janssens-Maenhout, G., Crippa, M., Guizzardi, D., Dentener, F., Muntean, M., Pouliot, G., Keating, T., Zhang,
435   Q., Kurokawa, J., Wankmüller, R., Denier van der Gon, H., Kuenen, J. J. P., Klimont, Z., Frost, G., Darras,
S., Koffi, B., and Li, M.: HTAP_v2.2: a mosaic of regional and global emission grid maps for 2008 and 2010
to study hemispheric transport of air pollution, Atmos. Chem. Phys., 15, 11 411–11 432, doi:10.5194/acp-
15-11411-2015, http://www.atmos-chem-phys.net/15/11411/2015/, 2015.

Jensen, N. O. and Hummelshøj, P.: Derivation of canopy resistance for water vapour fluxes over a spruce forest,
440   using a new technique for the viscous sublayer resistance, Agric. For. Meteorol., 73, 339–352, 1995.

Jensen, N. O. and Hummelshøj, P.: Erratum, Agric. For. Meteorol., 85, 289, doi:10.1016/S0168-1923(97)00024-
5, http://www.sciencedirect.com/science/article/pii/S0168192397000245, 1997.

Johansson, O., Palmqvist, K., and Olofsson, J.: Nitrogen deposition drives lichen community changes through
differential species responses, Glob. Chang. Biol., 18, 2626–2635, 2012.

445   Kalnay, E., Kanamitsu, M., Kistler, R., Collins, W., Deaven, D., Gandin, L., Iredell, M., Saha, S., White, G.,
Woollen, J., Zhu, Y., Leetmaa, A., Reynolds, R., Chelliah, M., Ebisuzaki, W., Higgins, W., Janowiak, J., Mo,
K. C., Ropelewski, C., Wang, J., Jenne, R., and Joseph, D.: The NCEP/NCAR 40-Year Reanalysis Project,
Bull. Am. Meteorol. Soc., 77, 437–471, 1996.

Lamarque, J.-F., Kyle, G., Meinshausen, M., Riahi, K., Smith, S., van Vuuren, D., Conley, A., and Vitt, F.:
450   Global and regional evolution of short-lived radiatively-active gases and aerosols in the Representative Con-
centration Pathways, Clim. Change, 109, 191–212, 10.1007/s10584-011-0155-0, 2011.

Lamarque, J.-F., Dentener, F., McConnell, J., Ro, C.-U., Shaw, M., Vet, R., Bergmann, D., Cameron-Smith,
P., Dalsoren, S., Doherty, R., Faluvegi, G., Ghan, S. J., Josse, B., Lee, Y. H., MacKenzie, I. A., Plummer,
D., Shindell, D. T., Skeie, R. B., Stevenson, D. S., Strode, S., Zeng, G., Curran, M., Dahl-Jensen, D., Das,
455   S., Fritzsche, D., and Nolan, M.: Multi-model mean nitrogen and sulfur deposition from the Atmospheric
Chemistry and Climate Model Intercomparison Project (ACCMIP): evaluation of historical and projected
future changes, Atmos. Chem. Phys., 13, 7997–8018, 2013.

Latysh, N. and Wetherbee, G.: Improved mapping of National Atmospheric Deposition Program wet-deposition
in complex terrain using PRISM-gridded data sets, Environ. Monit. Assess., 184, 913–928, 10.1007/s10661-
460   011-2009-7, 2012.

Lehmann, C. M., Bowersox, V. C., and Larson, S. M.: Spatial and temporal trends of precipitation chemistry in
the United States, 1985–2002, Environ. Pollut., 135, 347–361, 2005.

Lepori, F. and Keck, F.: Effects of Atmospheric Nitrogen Deposition on Remote Freshwater Ecosystems, Ambio, 41, 235–246, doi:10.1007/s13280-012-0250-0, http://www.ncbi.nlm.nih.gov/pmc/articles/
465   PMC3357855/, 2012.

Leuning, R.: A critical appraisal of a combined stomatal-photosynthesis model for C3 plants, Plant, Cell & Environment, 18, 339–355, 1995.

Levy, H., Horowitz, L. W., Schwarzkopf, M. D., Ming, Y., Golaz, J.-C., Naik, V., and Ramaswamy, V.: The roles of aerosol direct and indirect effects in past and future climate change, J. Geophys. Res. Atmos., 118,
470   4521–4532, 2013.

Li, Y., Schichtel, B. A., Walker, J. T., Schwede, D. B., Chen, X., Lehmann, C. M. B., Puchalski, M. A., Gay, D. A., and Collett, J. L.: Increasing importance of deposition of reduced nitrogen in the United States, Proc. Natl. Acad. Sci. U.S.A., p. 201525736, doi:10.1073/pnas.1525736113, http://www.pnas.org/content/early/2016/05/04/1525736113, 2016.

475 Loubet, B., Cellier, P., Milford, C., and Sutton, M. A.: A coupled dispersion and exchange model for short-range dry deposition of atmospheric ammonia, Quart. J. Roy. Meteor. Soc., 132, 1733–1763, 2006.

Magnani, F., Mencuccini, M., Borghetti, M., Berbigier, P., Berninger, F., Delzon, S., Grelle, A., Hari, P., Jarvis, P. G., Kolari, P., Kowalski, A. S., Lankreijer, H., Law, B. E., Lindroth, A., Loustau, D., Manca, G., Moncrieff, J. B., Rayment, M., Tedeschi, V., Valentini, R., and Grace, J.: The human footprint in the carbon cycle of
480   temperate and boreal forests, Nature, 447, 849–851, 2007.

Malm, W. C., Rodriguez, M. A., Schichtel, B. A., Gebhart, K. A., Thompson, T. M., Barna, M. G., Benedict, K. B., Carrico, C. M., and Collett Jr., J. L.: A hybrid modeling approach for estimating reactive nitrogen deposition in Rocky Mountain National Park, Atmos. Environ., 126, 258–273, doi:10.1016/j.atmosenv.2015.11.060, http://www.sciencedirect.com/science/article/pii/
485   S1352231015305677, 2016.

Malyshev, S., Shevliakova, E., Stouffer, R. J., and Pacala, S. W.: Contrasting Local versus Regional Effects of Land-Use-Change-Induced Heterogeneity on Historical Climate: Analysis with the GFDL Earth System Model, J. Clim., 28, 5448–5469, 2015.

Massad, R.-S., Nemitz, E., and Sutton, M. A.: Review and parameterisation of bi-directional ammonia exchange
490   between vegetation and the atmosphere, Atmos. Chem. Phys., 10, 10 359–10 386, 2010.

Matsuda, K., Watanabe, I., Wingpud, V., Theramongkol, P., and Ohizumi, T.: Deposition velocity of O_3 and SO_2 in the dry and wet season above a tropical forest in northern Thailand, Atmos. Environ., 40, 7557–7564, 2006.

Matt, D. R., McMillen, R. T., Womack, J. D., and Hicks, B. B.: A comparison of estimated and measured SO2
495   deposition velocities, Water. Air. Soil Pollut., 36, 331–347, doi:10.1007/BF00229676, http://link.springer.com.ezproxy.princeton.edu/article/10.1007/BF00229676, 1987.

Meunier, C. L., Gundale, M. J., Sánchez, I. S., and Liess, A.: Impact of nitrogen deposition on forest and lake food webs in nitrogen-limited environments, Glob. Chang. Biol., 22, 164–179, doi:10.1111/gcb.12967, http://onlinelibrary.wiley.com/doi/10.1111/gcb.12967/abstract, 2016.

500 Meyers, T., Finkelstein, P., Clarke, J., Ellestad, T., and Sims, P.: A multilayer model for inferring dry deposition using standard meteorological measurements, Journal of Geophysical Research-Atmospheres, 103, 22 645–22 661, 1998.

Milly, P. C. D., Malyshev, S. L., Shevliakova, E., Dunne, K. A., Findell, K. L., Gleeson, T., Liang, Z., Phillipps, P., Stouffer, R. J., and Swenson, S.: An Enhanced Model of Land Water and Energy for Global Hydrologic and Earth-System Studies, J. Hydrometeorol., 15, 1739–1761, 2014.

Myles, L., Heuer, M. W., Meyers, T. P., and Hoyett, Z. J.: A comparison of observed and parameterized SO_2 dry deposition over a grassy clearing in Duke Forest, Atmos. Environ., 49, 212–218, 2012.

Naik, V., Horowitz, L. W., Fiore, A. M., Ginoux, P., Mao, J., Aghedo, A. M., and Levy, H.: Impact of preindustrial to present-day changes in short-lived pollutant emissions on atmospheric composition and climate forcing, J. Geophys. Res. Atmos., 118, 8086–8110, 2013.

Neirynck, J., Flechard, C. R., and Fowler, D.: Long-term (13 years) measurements of SO_2 fluxes over a forest and their control by surface chemistry, Agric. For. Meteorol., 151, 1768–1780, 2011.

Nemitz, E., Milford, C., and Sutton, M. A.: A two-layer canopy compensation point model for describing bi-directional biosphere-atmosphere exchange of ammonia, Quart. J. Roy. Meteor. Soc., 127, 815–833, 2001.

Nguyen, T. B., Crounse, J. D., Teng, A. P., Clair, J. M. S., Paulot, F., Wolfe, G. M., and Wennberg, P. O.: Rapid deposition of oxidized biogenic compounds to a temperate forest, Proc. Natl. Acad. Sci. U.S.A., 112, E392–E401, doi:10.1073/pnas.1418702112, http://www.pnas.org/content/112/5/E392, 2015.

Ochoa-Hueso, R., Allen, E. B., Branquinho, C., Cruz, C., Dias, T., Fen, M. E., Manrique, E., Pérez-Corona, M. E., Sheppard, L. J., and Stock, W. D.: Nitrogen deposition effects on Mediterranean-type ecosystems: An ecological assessment, Environ. Pollut., 159, 2265 – 2279, 2011.

Otoshi, T., Fukuzaki, N., Li, H., Hoshino, H., Sase, H., Saito, M., and Suzuki, K.: Quality Control and Its Constraints during the Preparatory-Phase Activities of the Acid Deposition Monitoring Network in East Asia (EANET), Water. Air. Soil Pollut., 130, 1613–1618, doi:10.1023/A:1013905029034, http://link.springer.com/article/10.1023/A%3A1013905029034, 2001.

Pardo, L. H., Fenn, M. E., Goodale, C. L., Geiser, L. H., Driscoll, C. T., Allen, E. B., Baron, J. S., Bobbink, R., Bowman, W. D., Clark, C. M., Emmett, B., Gilliam, F. S., Greaver, T. L., Hall, S. J., Lilleskov, E. A., Liu, L., Lynch, J. A., Nadelhoffer, K. J., Perakis, S. S., Robin-Abbott, M. J., Stoddard, J. L., Weathers, K. C., and Dennis, R. L.: Effects of nitrogen deposition and empirical nitrogen critical loads for ecoregions of the United States, Ecol. Appl., 21, 3049–3082, 2011.

Paulot, F., Crounse, J. D., Kjaergaard, H. G., Kroll, J. H., Seinfeld, J. H., and Wennberg, P. O.: Isoprene photoox-idation: new insights into the production of acids and organic nitrates, Atmos. Chem. Phys., 9, 1479–1501, 2009.

Paulot, F., Jacob, D. J., and Henze, D. K.: Sources and Processes Contributing to Nitrogen Deposition: An Adjoint Model Analysis Applied to Biodiversity Hotspots Worldwide, Environ. Sci. Technol., 47, 3226–3233, 2013.

Paulot, F., Jacob, D. J., Pinder, R. W., Bash, J. O., Travis, K., and Henze, D. K.: Ammonia emissions in the United States, European Union, and China derived by high-resolution inversion of ammonium wet deposition data: Interpretation with a new agricultural emissions inventory (MASAGE_NH3), J. Geophys. Res. Atmos., 119, 4343–4364, 2014.

Paulot, F., Ginoux, P., Cooke, W. F., Donner, L. J., Fan, S., Lin, M.-Y., Mao, J., Naik, V., and Horowitz, L. W.: Sensitivity of nitrate aerosols to ammonia emissions and to nitrate chemistry: implications for present and

future nitrate optical depth, Atmos. Chem. Phys., 16, 1459–1477, doi:10.5194/acp-16-1459-2016, http://www.atmos-chem-phys.net/16/1459/2016/, 2016.

Paulot, F., Fan, S., and Horowitz, L. W.: Contrasting seasonal responses of sulfate aerosols to declining SO_2
545 emissions in the Eastern U.S.: Implications for the efficacy of SO_2 emission controls, Geophys. Res. Lett., 44, 455–464, doi:10.1002/2016GL070695, http://dx.doi.org/10.1002/2016GL070695, 2016GL070695, 2017.

Phoenix, G. K., Emmett, B. A., Britton, A. J., Caporn, S. J. M., Dise, N. B., Helliwell, R., Jones, L., Leake, J. R., Leith, I. D., Sheppard, L. J., Sowerby, A., Pilkington, M. G., Rowe, E. C., Ashmore, M. R., and Power, S. A.: Impacts of atmospheric nitrogen deposition: responses of multiple plant and soil parameters across
550 contrasting ecosystems in long-term field experiments, Glob. Chang. Biol., 18, 1197–1215, 2012.

Ponette-González, A. G., Weathers, K. C., and Curran, L. M.: Tropical land-cover change alters biogeochemical inputs to ecosystems in a Mexican montane landscape, Ecol. Appl., 20, 1820–1837, 2010.

Portmann, F. T., Siebert, S., and Döll, P.: MIRCA2000 — Global monthly irrigated and rainfed crop areas around the year 2000: A new high-resolution data set for agricultural and hydrological modeling, Global
555 Biogeochem. Cycles, 24, GB1011, 2010.

Pregitzer, K. S., Burton, A. J., Zak, D. R., and Talhelm, A. F.: Simulated chronic nitrogen deposition increases carbon storage in Northern Temperate forests, Global Change Biol., 14, 142–153, 2008.

Ran, L., Pleim, J., Song, C., Band, L., Walker, J. T., and Binkowski, F. S.: A photosynthesis-based two-leaf canopy stomatal conductance model for meteorology and air quality modeling with WRF/CMAQ PX LSM,
560 Journal of Geophysical Research: Atmospheres, 122, 1930–1952, doi:10.1002/2016jd025583, https://doi.org/10.1002/2016jd025583, 2017.

Reay, D. S., Dentener, F., Smith, P., Grace, J., and Feely, R. A.: Global nitrogen deposition and carbon sinks, Nat. Geosci., 1, 430–437, 2008.

Riahi, K., Rao, S., Krey, V., Cho, C., Chirkov, V., Fischer, G., Kindermann, G., Nakicenovic, N., and Rafaj, P.:
565 RCP 8.5—A scenario of comparatively high greenhouse gas emissions, Clim. Chang., 109, 33–57, 2011.

Rienecker, M. M., Suarez, M. J., Gelaro, R., Todling, R., Bacmeister, J., Liu, E., Bosilovich, M. G., Schubert, S. D., Takacs, L., Kim, G.-K., Bloom, S., Chen, J., Collins, D., Conaty, A., da Silva, A., Gu, W., Joiner, J., Koster, R. D., Lucchesi, R., Molod, A., Owens, T., Pawson, S., Pegion, P., Redder, C. R., Reichle, R., Robert-son, F. R., Ruddick, A. G., Sienkiewicz, M., and Woollen, J.: MERRA: NASA's Modern-Era Retrospective
570 Analysis for Research and Applications, J. Clim., 24, 3624–3648, 2011.

Sanderson, M. G., Collins, W. J., Hemming, D. L., and Betts, R. A.: Stomatal conductance changes due to increasing carbon dioxide levels: Projected impact on surface ozone levels, Tellus B, 59, doi:10.3402/tellusb.v59i3.17002, http://www.tellusb.net/index.php/tellusb/article/view/17002, 2007.

Schwede, D. B. and Lear, G. G.: A novel hybrid approach for estimating total deposition in the United States,
575 Atmos. Environ., 92, 207–220, 2014.

Sheppard, L. J., Leith, I. D., Mizunuma, T., Neil Cape, J., Crossley, A., Leeson, S., Sutton, M. A., van Dijk, N., and Fowler, D.: Dry deposition of ammonia gas drives species change faster than wet deposition of ammonium ions: evidence from a long-term field manipulation, Glob. Chang. Biol., 17, 3589–3607, doi:10.1111/j.1365-2486.2011.02478.x, http://onlinelibrary.wiley.com/doi/10.1111/j.
580 1365-2486.2011.02478.x/abstract, 2011.

Shevliakova, E., Pacala, S. W., Malyshev, S., Hurtt, G. C., Milly, P. C. D., Caspersen, J. P., Sentman, L. T., Fisk, J. P., Wirth, C., and Crevoisier, C.: Carbon cycling under 300 years of land use change: Importance of the secondary vegetation sink, Global Biogeochem. Cycles, 23, GB2022, 2009.

Simkin, S. M., Allen, E. B., Bowman, W. D., Clark, C. M., Belnap, J., Brooks, M. L., Cade, B. S., Collins, S. L., Geiser, L. H., Gilliam, F. S., Jovan, S. E., Pardo, L. H., Schulz, B. K., Stevens, C. J., Suding, K. N., Throop, H. L., and Waller, D. M.: Conditional vulnerability of plant diversity to atmospheric nitrogen deposition across the United States, Proc. Natl. Acad. Sci. U.S.A., 113, 4086–4091, doi:10.1073/pnas.1515241113, http://www.pnas.org/content/113/15/4086, 2016.

Simpson, D., Fagerli, H., Jonson, J., Tsyro, S., Wind, P., and Tuovinen, J.: The EMEP Unified Eulerian Model. Model Description. EMEP MSC-W Report 12003, The Norwegian Meteorological Institute, Oslo, Norway, 2003.

Smith, B., Wårlind, D., Arneth, A., Hickler, T., Leadley, P., Siltberg, J., and Zaehle, S.: Implications of incorporating N cycling and N limitations on primary production in an individual-based dynamic vegetation model, Biogeosciences, 11, 2027–2054, doi:10.5194/bg-11-2027-2014, https://doi.org/10.5194/bg-11-2027-2014, 2014.

Sorimachi, A., Sakamoto, K., Ishihara, H., Fukuyama, T., Utiyama, M., Liu, H., Wang, W., Tang, D., Dong, X., and Quan, H.: Measurements of sulfur dioxide and ozone dry deposition over short vegetation in northern China—a preliminary study, Atmos. Environ., 37, 3157–3166, 2003.

Stevens, C. J., Dise, N. B., Mountford, J. O., and Gowing, D. J.: Impact of Nitrogen Deposition on the Species Richness of Grasslands, Science, 303, 1876–1879, 2004.

Storkey, J., Macdonald, A. J., Poulton, P. R., Scott, T., Köhler, I. H., Schnyder, H., Goulding, K. W. T., and Crawley, M. J.: Grassland biodiversity bounces back from long-term nitrogen addition, Nature, 528, 401–404, doi:10.1038/nature16444, http://www.nature.com/nature/journal/v528/n7582/abs/nature16444.html, 2015.

Sutton, M. A., Simpson, D., Levy, P. E., Smith, R. I., Reis, S., Van Oijen, M., and De Vries, W.: Uncertainties in the relationship between atmospheric nitrogen deposition and forest carbon sequestration, Glob. Chang. Biol., 14, 2057–2063, 2008.

Sutton, M. A., Howard, C. M., Erisman, J. W., Billen, G., Bleeker, A., Grennfelt, P., Grinsven, H. v., and Grizzetti, B., eds.: The European Nitrogen Assessment: Sources, Effects and Policy Perspectives, Cambridge University Press, 2011.

Templer, P. H., Weathers, K. C., Lindsey, A., Lenoir, K., and Scott, L.: Atmospheric inputs and nitrogen saturation status in and adjacent to Class I wilderness areas of the northeastern US, Oecologia, 177, 5–15, 2014.

Townsend, A. R., Braswell, B. H., Holland, E. A., and Penner, J. E.: Spatial and Temporal Patterns in Terrestrial Carbon Storage Due to Deposition of Fossil Fuel Nitrogen, Ecol. Appl., 6, 806–814, 1996.

van Vuuren, D., Edmonds, J., Kainuma, M., Riahi, K., Thomson, A., Hibbard, K., Hurtt, G., Kram, T., Krey, V., Lamarque, J.-F., Masui, T., Meinshausen, M., Nakicenovic, N., Smith, S., and Rose, S.: The representative concentration pathways: an overview, Clim. Change, 109, 5–31, 2011.

Wang, Y., Jacob, D. J., and Logan, J. A.: Global simulation of tropospheric O_3-NO_x-hydrocarbon chemistry 1. Model formulation, J. Geophys. Res., 103, 10 713–10 726, 1998.

620   Wårlind, D., Smith, B., Hickler, T., and Arneth, A.: Nitrogen feedbacks increase future terrestrial ecosystem
       carbon uptake in an individual-based dynamic vegetation model, Biogeosciences, 11, 6131–6146, 2014.

Weathers, K. C., Lovett, G. M., Likens, G. E., and Lathrop, R.: The Effect of Landscape Features on Deposition
       to Hunter Mountain, Catskill Mountains, New York, Ecol. Appl., 10, 528–540, doi:10.2307/2641112, http:
       //www.jstor.org/stable/2641112, 2000.

625   Weathers, K. C., Simkin, S. M., Lovett, G. M., and Lindberg, S. E.: Empirical Modeling of Atmospheric Depo-
       sition in Mountainous Landscapes, Ecol. Appl., 16, 1590–1607, 2006.

Wentworth, G. R., Murphy, J. G., Benedict, K. B., Bangs, E. J., and Collett Jr., J. L.: The role of dew as a
       night-time reservoir and morning source for atmospheric ammonia, Atmos. Chem. Phys., 16, 7435–7449,
       doi:10.5194/acp-16-7435-2016, http://www.atmos-chem-phys.net/16/7435/2016/, 2016.

630   Wesely, M. . L.: Parameterization of surface resistances to gaseous dry deposition in regional-scale numerical
       models, Atmos. Environ., 23, 1293–1304, 1989.

Williams, J. J., Chung, S. H., Johansen, A. M., Lamb, B. K., Vaughan, J. K., and Beutel, M.: Evaluation of atmo-
       spheric nitrogen deposition model performance in the context of U.S. critical load assessments, Atmospheric
       Environment, 150, 244–255, doi:10.1016/j.atmosenv.2016.11.051, https://doi.org/10.1016/j.atmosenv.2016.
635   11.051, 2017.

Wolfe, A. P., Van Gorp, A. C., and Baron, J. S.: Recent ecological and biogeochemical changes in alpine
       lakes of Rocky Mountain National Park (Colorado, USA): a response to anthropogenic nitrogen deposition,
       Geobiology, 1, 153–168, 2003.

Wu, W. and Driscoll, C. T.: Impact of Climate Change on Three-Dimensional Dynamic Critical Load Functions,
640   Environ. Sci. Technol., 44, 720–726, pMID: 20020745, 2010.

Wu, Z., Staebler, R., Vet, R., and Zhang, L.: Dry deposition of O_3 and SO_2 estimated from gradient measure-
       ments above a temperate mixed forest, Environ. Pollut., 210, 202–210, doi:10.1016/j.envpol.2015.11.052,
       http://www.sciencedirect.com/science/article/pii/S0269749115302128, 2016.

Wu, Z., Schwede, D. B., Vet, R., Walker, J. T., Shaw, M., Staebler, R., and Zhang, L.: Evaluation and inter-
645   comparison of five North American dry deposition algorithms at a mixed forest site, Journal of Advances in
       Modeling Earth Systems, doi:10.1029/2017ms001231, https://doi.org/10.1029/2017ms001231, 2018.

Zaehle, S., Friend, A. D., Friedlingstein, P., Dentener, F., Peylin, P., and Schulz, M.: Carbon and nitrogen cycle
       dynamics in the O-CN land surface model: 2. Role of the nitrogen cycle in the historical terrestrial carbon
       balance, Global Biogeochemical Cycles, 24, n/a–n/a, doi:10.1029/2009gb003522, https://doi.org/10.1029/
650   2009gb003522, 2010.

Zhang, L., Gong, S., Padro, J., and Barrie, L.: A size-segregated particle dry deposition scheme for an atmo-
       spheric aerosol module, Atmos. Environ., 35, 549–560, 2001.

Zhang, L., Moran, M. D., Makar, P. A., Brook, J. R., and Sunling, G.: Modelling gaseous dry deposition in
       AURAMS: a unified regional air-quality modelling system, Atmos. Environ., 36, 537—560, 2002.

655   Zhang, L., Brook, J. R., and Vet, R.: A revised parameterization for gaseous dry deposition in air-quality models,
       Atmos. Chem. Phys., 3, 2067–2082, 2003.

Zhang, L., Jacob, D. J., Knipping, E. M., Kumar, N., Munger, J. W., Carouge, C. C., van Donkelaar, A., Wang,
       Y. X., and Chen, D.: Nitrogen deposition to the United States: distribution, sources, and processes, Atmos.
       Chem. Phys., 12, 4539–4554, 2012.